Integrated Photonics Research Conference, Santa Barbara, July 1999

Efficiency Analysis of Quantum Well Lasers using PICS3D

Joachim Piprek, Patrick Abraham, and John E. Bowers
Electrical and Computer Engineering Department
University of California, Santa Barbara, CA 93106-9560
Phone: 805-893-4051, Fax: 805-893-5440, E-mail: piprek@ece.ucsb.edu

The performance of multi-quantum well (MQW) laser diodes is often limited by loss mechanisms. Only the fraction η_i of carriers injected above threshold generates stimulated photons. The rest is lost in carrier leakage or non-stimulated recombination within the active region (Shockley-Read-Hall recombination, spontaneous recombination, or Auger recombination). Only the fraction η_o of stimulated photons ends up in the emitted laser beam. Both the internal differential efficiency η_i and the optical efficiency η_o determine the measured slope efficiency $\eta_d = \eta_i\eta_o$ of the power vs. current P(I) characteristic. The different carrier loss mechanisms are hard to distinguish by experimental methods. However, it is of great importance for laser optimization to identify the mechanisms that limit the performance of actual devices. We demonstrate such an analysis of measurements using quasi three-dimensional (3D) numerical laser simulation.

Laser simulation codes have been developed by several research groups and commercial laser software has entered the market. PICS3D [1] is one of the most advanced packages in this field. It self-consistently combines two-dimensional carrier transport, wave guiding, and gain calculations with a longitudinal mode solver. Using commercial software has the advantage that results can be reproduced and extended by other researchers.

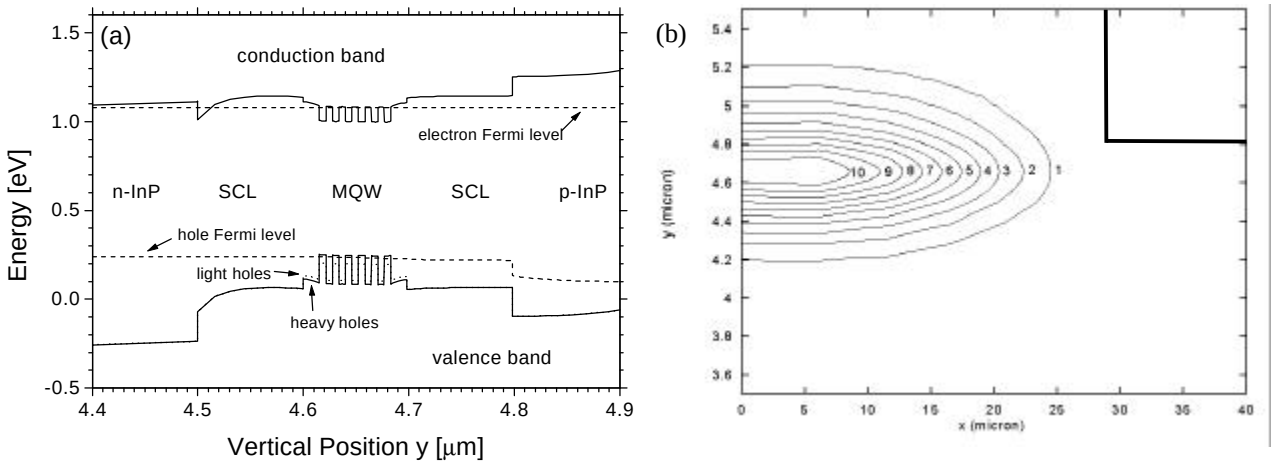

Fig. 1: (a) Energy band diagram of the active region. (b) Normalized wave intensity at the laser facet (y – vertical position, x – lateral distance from y-axis).

In this paper, we focus on the analysis of loss mechanisms in 1.55μm InGaAsP/InP ridge-waveguide laser diodes (Fig. 1). The laser structures are grown by metalorganic vapor phase epitaxy. The MQW active

region consists of six compressively strained (1%) $In_{0.76}Ga_{0.24}As_{0.79}P_{0.21}$ quantum wells and $In_{0.71}Ga_{0.29}As_{0.55}P_{0.45}$ barriers. The MQW stack is sandwiched between 100nm thick InGaAsP separate confinement layers (SCLs). Broad area ridge-waveguide lasers (57μm wide ridge) are processed with the p-ridge etched down to the SCL layer. Energy band diagram and wave intensity at the laser facet are shown in Fig. 1. Lasers with different cavity length are manufactured and characterized as-cleaved. Pulsed power vs. current P(I) measurements with different cavity lengths L and with different stage temperatures T are shown in Fig. 2 (dots).

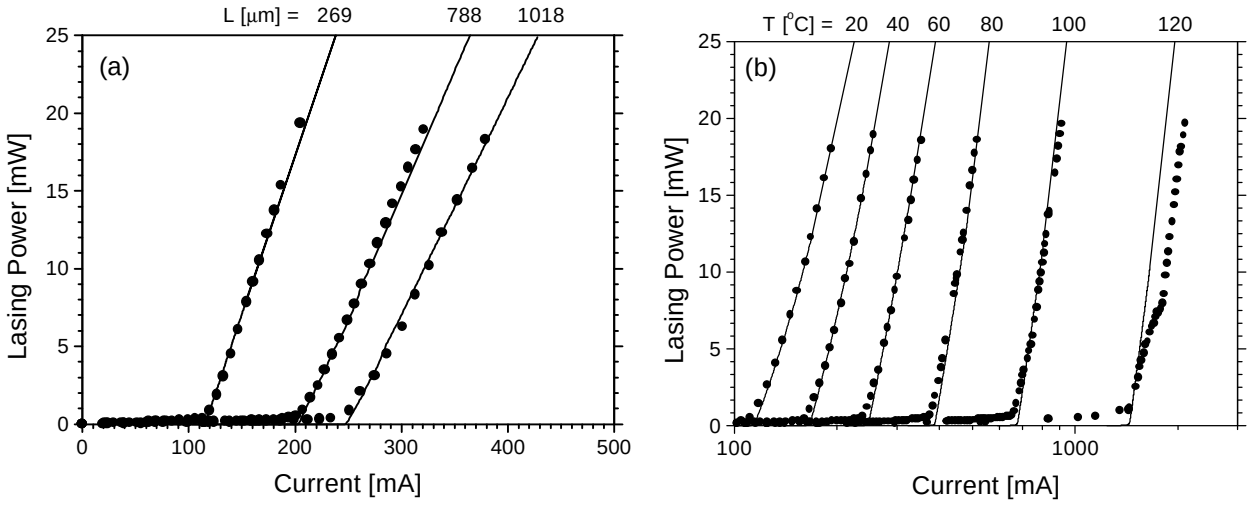

Fig. 2: Pulsed power vs. current characteristics (a) for various laser lengths L at T=20°C and (b) for various stage temperatures T with L=269μm. Dots give measurements and lines give simulation results.

Linear fits to the inverse slope efficiencies $1/\eta_d(L)$ from Fig. 2a are used to extract the internal differential efficiency $\eta_i = 0.67$ and the internal optical absorption $\alpha_i = 14cm^{-1}$. Since both the loss parameters depend on the cavity length, this method may not give accurate results for short lasers. Measured temperature effects on threshold current $I_{th}(T)$ and slope efficiency $\eta_d(T)$ are often described by characteristic temperatures T_o and T_η, respectively. From Fig. 2b, we find that both parameters show a monotonic decrease with increasing temperature: T_o = 55…20K, T_η = 180…30K. This simple analysis does not reveal the physical mechanisms behind all these parameters.

PICS3D includes models for all relevant loss mechanisms and a fit to measurements can usually be obtained by careful adjustment of material parameters. However, the correct balance of all physical mechanisms is only found when a variety of measurements is reproduced simultaneously using the same set of material parameters. For our lasers, Fig. 2 demonstrates an excellent agreement of simulation (lines) and experiment (dots). To achieve this, several key parameters had to be identified and adjusted. Internal optical losses are governed by the material parameter κ which gives the local absorption $\kappa_p p+\kappa_n n$ as function of the local carrier densities (n – electrons, p – holes). This parameter includes free carrier absorption as well as intervalence band absorption (IVBA). Holes are assumed to dominate absorption and $\kappa_p = 120 \times 10^{-18}$ cm^2 is obtained from the fit in Fig. 2a. This result is in good agreement with published absorption measurements [2]. Carrier losses are dominated by the Auger recombination rate $np(C_p p+C_n n)$

which is assumed to be governed by the conduction-hole-hole-split-off (CHHS) process. In good agreement with the literature, a room-temperature Auger parameter of $C_p = 1.6 \times 10^{-28}$ $cm^{-6}s^{-1}$ is extracted with an Arrhenius-type temperature dependence (activation energy ΔE_a=60meV).

Auger recombination is not only the strongest contribution to the threshold current $I_{th}(T)$, it also affects our differential internal efficiency $\eta_i=\eta_s\eta_e\eta_r$ which can be separated into contributions from lateral spreading current (η_s), vertical carrier escape from the active region (η_e), and recombination losses within the active region (η_r) [3]. Fig. 3a shows the calculated MQW electron density n(x,y) at the laser facet indicating lateral carrier leakage. An enhancement of recombination losses above threshold ($\eta_r<1$) is often neglected assuming QW carrier density clamping. We recently showed that increasing non-uniformity of the MQW carrier distribution yields enhanced Auger recombination above threshold causing η_r to limit the differential internal efficiency of our lasers [4]. At room temperature, we obtain η_e=0.99, η_s=0.90, and η_r=0.74 giving η_i=0.66 which is in excellent agreement with the $1/\eta_d(L)$ measurement. Temperature effects on carrier loss mechanisms are shown in Fig. 3b. Carrier spreading slightly declines due to the lower mobility at higher temperature. MQW recombination losses slightly increase but they loose their dominating role to vertical carrier leakage at about 80°C. The escape of electrons into the p-InP cladding layer dominates the strong reduction of the slope efficiency $\eta_d(T)$ at higher temperatures.

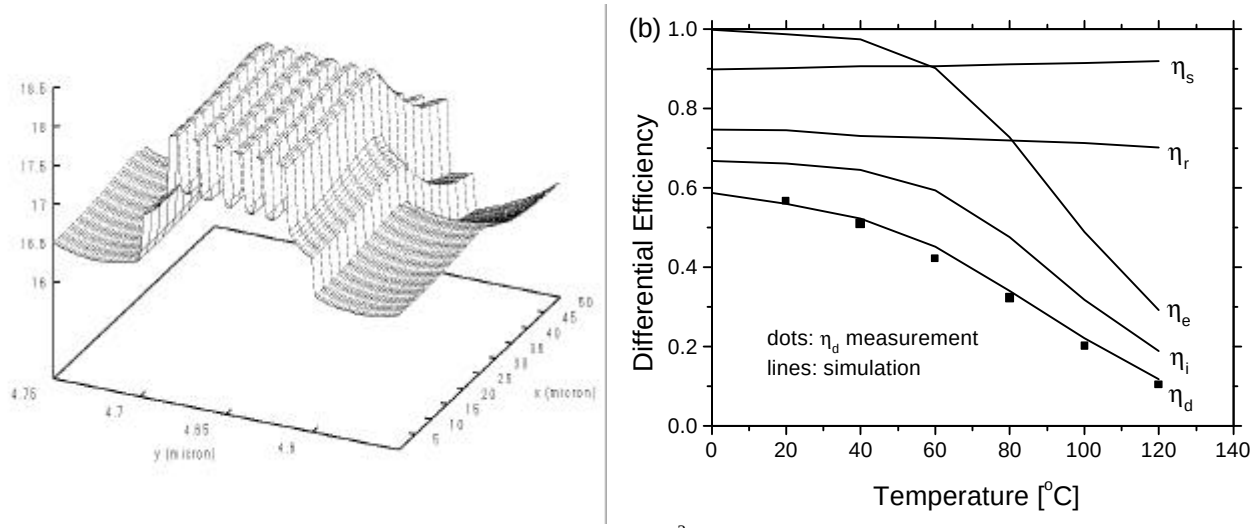

Fig. 3: (a) Logarithm of MQW electron density n(x,y) [cm^{-3}] at laser facet (y – vertical position, x – lateral distance from y-axis). (b) Differential efficiencies vs. stage temperature (see text).

[1] PICS3D 4.1.2 by Crosslight Software, Inc., 1998 (details are available at www.crosslight.ca).
[2] I. Joindot and J. L. Beylat, Electr. Lett. **29**, 604 (1993).
[3] P.M. Smowton and P. Blood, IEEE J. Sel. Top. Quant. Electr. **3**, 491 (1997).
[4] J. Piprek, P. Abraham, and J. E. Bowers, Appl. Phys. Lett. **74**, 489 (1999).